Z' identification at the HE-LHC

Clement Helsens[1], David Jamin[2], Michelangelo L. Mangano[3], Thomas G. Rizzo[4], and Michele Selvaggi[1]

[1]CERN EP-Departement, CH-1211 Geneva 23, Switzerland
[2]Academia Sinica, Institute of Physics, Taipei, Taiwan
[3]CERN TH-Departement, CH-1211 Geneva 23, Switzerland
[4]SLAC National Accelerator Laboratory 2575 Sand Hill Rd., Menlo Park, CA, 94025 USA

September 28, 2018

Contents

Abstract

The 14 TeV LHC with L=3 ab^{-1} of integrated luminosity can search for new Z' gauge bosons from the classic extended gauge theories up to masses of roughly $\simeq$ 6 TeV. Here we analyzed the capability of the 27 TeV HE-LHC with L=15 ab^{-1} to distinguish among six Z' models employing only the e^+e^- and $\mu^+\mu^-$ channels assuming that $M_{Z'} = 6$ TeV. Under the assumption that these

Z''s decay only to SM particles, we show that there are sufficient observables to perform this model differentiation in most cases.

1 Context of the study

It is legitimate to assume that a heavy resonance could be seen at the end of High Luminosity LHC (HL-HLC). If that is the case a new collider with higher energy in the center of mass is needed to study its property as not enough events will be available at 14 TeV. In this document we present the discrimination potential of a High Energy LHC (HE-LHC) with an assumed center of mass energy of 27 TeV.

2 Bounds from HL-LHC

As a starting point it is needed to understand what are, for $\sqrt{s}$ = 14 TeV, for the typical exclusion/discovery reaches for some standard reference Z' models assuming L=3 ab^{-1} employing only the e^+e^- and $\mu^+\mu^-$ channels. To address this and the other questions below we will use the same set of Z' models as employed in [1] and mostly in [2], both of which we will refer to frequently. We employ the MMHT2014 NNLO set [3] throughout with an appropriate constant K-factor (=1.27) for numerics. The upper panel in Fig. 1 shows the production cross section times leptonic BF for these models at 14 TeV in the NWA. It has been and will be assumed here that these Z' states only decay to SM particles.

Using the present ATLAS and CMS results at 13 TeV, [4] and [5], it is straightforward to estimate by extrapolation the eventual 14 TeV exclusion reach in the combined $e + \mu$ sample; this is given in the first column of Table 1. For discovery, only the e channel is used due to poor μ-pair mass resolution near $M_{Z'} = 6$ TeV although the muons will add some additional support for any observed excess as large masses. Estimates of the 3σ evidence and 5σ discovery limits are also given in the Table. Based on these results, we will assume in our study below that we are dealing with a Z' of mass 6 TeV; somewhat smaller mass choices will lead to very similar conclusions based on the ratio of predicted event rates shown in the lower panel of Fig. 1. Fig.2 shows the NWA cross sections for the same set of models but now at 27 TeV; with L=15 ab^{-1}, we note that very large statistical samples will be available for the case of $M_{Z'} = 6$ TeV for each dilepton channel.

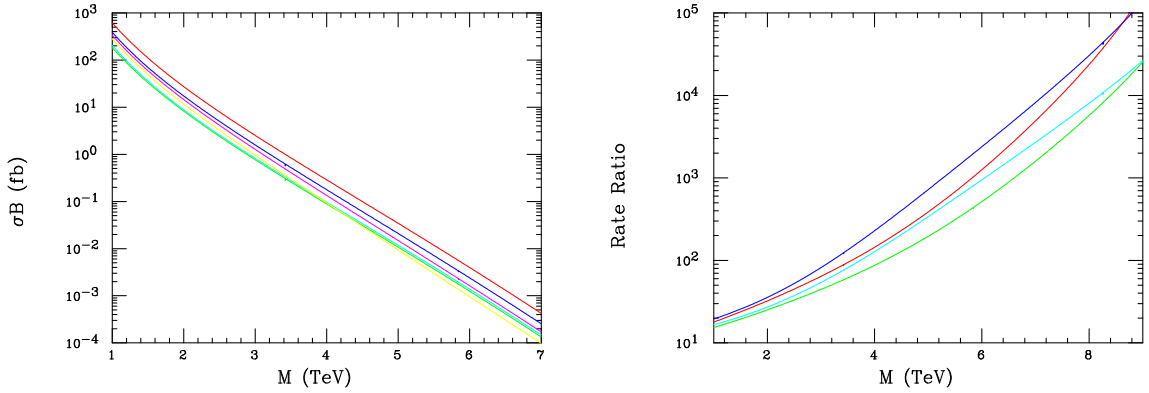

Figure 1: (Top) σB_l in the NWA for the Z' production at the $\sqrt{s} = 14$ TeV LHC as functions of the Z' mass: SSM(red), LRM (blue), ψ(green), χ(magenta), η(cyan), I(yellow). (Bottom) Ratio of the number of events for $\sqrt{s} = 27$ TeV, L=15 ab^{-1} to that at 13[14] TeV, L=3 ab^{-1} for $\bar{u}u$ (red) and $\bar{d}d$ (blue) [green, cyan] initial state partons with fixed invariant mass M.

Model	95% CL	3σ	5σ
SSM	6.62	6.09	5.62
LRM	6.39	5.85	5.39
ψ	6.10	5.55	5.07
χ	6.22	5.68	5.26
η	6.15	5.59	5.16
I	5.98	5.45	5.05

Table 1: $\sqrt{s} = 14$ TeV results for $M_{Z'}$ in TeV as discussed in the text.

3 Discrimination from direct calculations

Question: Can we use just this dilepton channel to distinguish between these six Z' models?

We make use of 3 observables, all in NWA: σB_l, the forward-backward asymmetry, A_{FB} and the rapidity ratio, r_y. These last two are defined and discussed at some extent in both [1] and [2]. Given the ATLAS and CMS analyses as presented in [6] and [7] we employ the entire range of rapidity $|y| \leq 2.5$ in defining these quantities. Based on these same works and [2], In addition to usual statistical errors, we will assume a 2% systematic error on the two ratios as most uncertainties (lumi and PDF) will cancel between numerators and denominators. For σB_l, we assign a 5% systematic error in addition to this 2%; all errors are then added in quadrature. I am aware that these may be aggressive numbers but the plots will tell all.

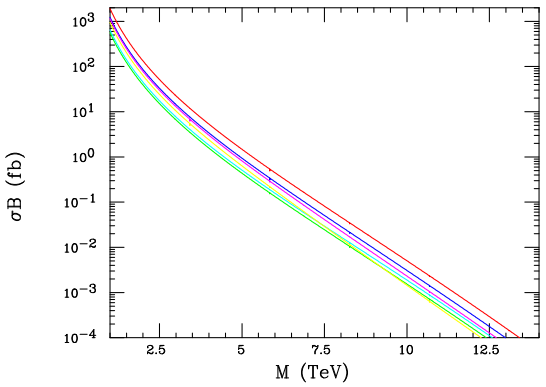

Figure 2: Same as the top panel in the previous Figure but now for the HE-LHC.

Fig. 3 shows the correlated predictions for these 3 observables for these six models given the above assumptions and employing *only* a single dilepton channel. Here we see that apart from a possible near degeneracy in models ψ, η, a reasonable Z' model separation is indeed achieved. It is clear that this remains possible even with somewhat larger values for the systematic errors. I note again that the use of σB_l relies on the absence of new non-SM decay modes.

4 Discrimination from detector level analysis

The analyses presented in this section are all performed within the FCC software framework, FCCSW [8]. The detector parametrisation considered in this study is from HE-LHC official parametrisation for the yellow report [9]. The Monte Carlo are first presented in Section 4.1 Leptonic decays are presented in 4.2, and hadronic analyses in 4.3.

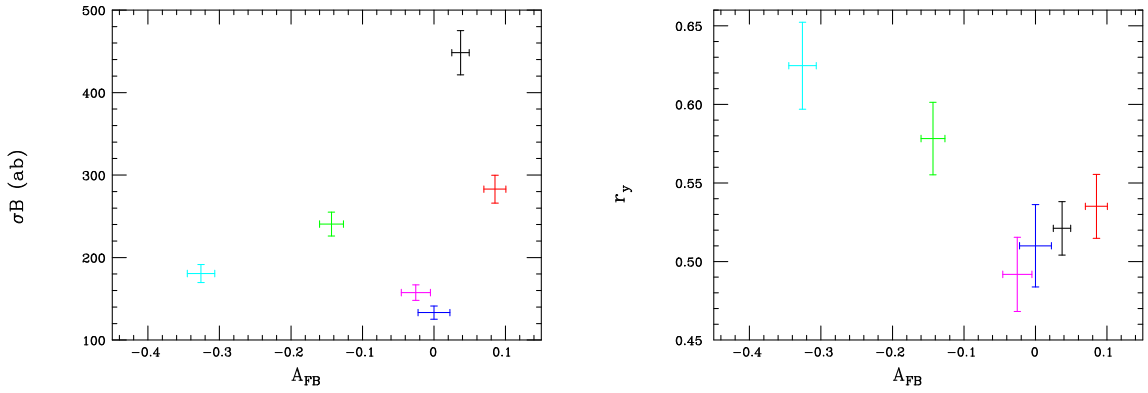

Figure 3: (Top) σB_l vs A_{FB} and (Bottom) r_y vs A_{FB} at the HE-LHC assuming $M'_Z = 6$ TeV as discussed in the text. SSM(black), LRM(red), ψ (blue), χ (green), η (magenta) and I (cyan). 1σ errors only are shown.

4.1 Monte Carlo Samples

Monte Carlo (MC) simulated event samples were used to simulate the response of the FCC detector to signal and backgrounds. The muon momentum resolution is assumed to be $\sigma(p)/p \approx 20\%$ at $p_{\mathrm{T}} = 20$TeV. Signals are generated with PYTHIA 8.230 [10] using the leading order cross-section from the generator. All lepton flavour decays of the Z' are generated assuming universality of the couplings. The Drell-Yan background has been generated using MG5_aMC@NLO 2.5.2 [11] at leading order only. A k-factor of 2 is applied to all the background processes.

4.2 Leptonic analysis

4.2.1 Event selection and discovery potential

Events are required to contain at least two same flavour leptons of opposite charge with $p_{\mathrm{T}} > 500$ GeV, $|\eta|$ <4.5. When mentioned a smaller acceptance of $|\eta|$ <2.5 is considered to test the impact on the reduction of the statistics. An additional cut on the di-lepton invariant mass $m_{ll} > 1$ TeV is applied to remove the low mass Drell-Yan. Figure 4 shows the invariant mass for a 6 TeV signal for the ee (left) and $\mu\mu$ channels (right). The mass resolution is better for the ee channel, as expected from the higher performance of the electro-magnetic calorimeter at high energy.

Limits and discovery potential for di-lepton resonances are shown in Figure 5. With the full 15 ab^{-1} integrated luminosity, it is expected to exclude heavy Z' resonances from 10 to 12.5 TeV depending on the model and discover a Z'_{SSM} up to 12 TeV.

4.2.2 Variables definition

As for the analysis from direct calculation, the observables are defined at the detector level. On Figure 6 the rapidity of the Z' is displayed, and as expected it is much more central for the signal than for the Drell-Yan background.

At detector level the variable r_y is defined as the ratio of central over forward events:

$$r_y = \frac{\sigma(|y_{Z'}| < y_1)}{\sigma(y_1 < |y_{Z'}| < y_2)} \tag{1}$$

with $y_1 = 0.5$ and $y_2 = 2.5$ for this study.

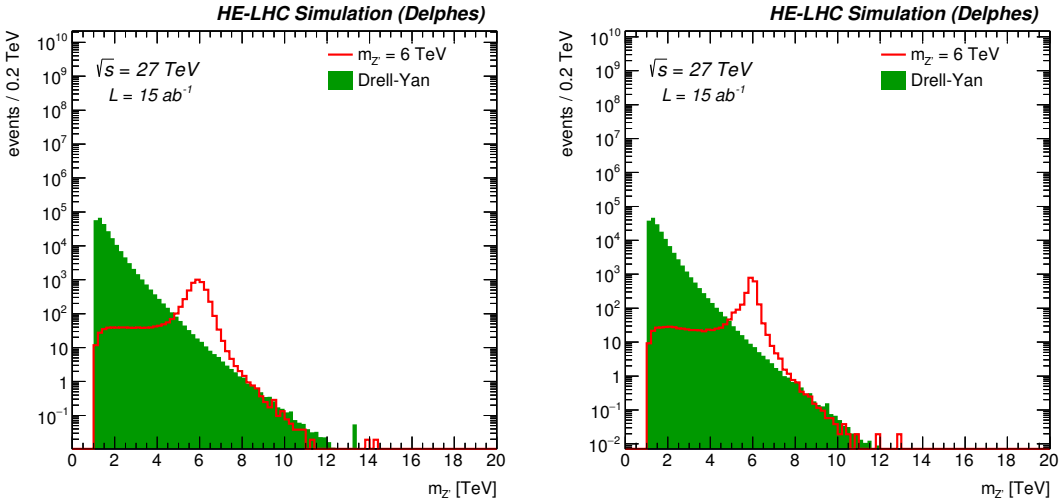

Figure 4: Invariant mass for a 6 TeV signal after full event selection for ee channel (left) and $\mu\mu$ channel (right).

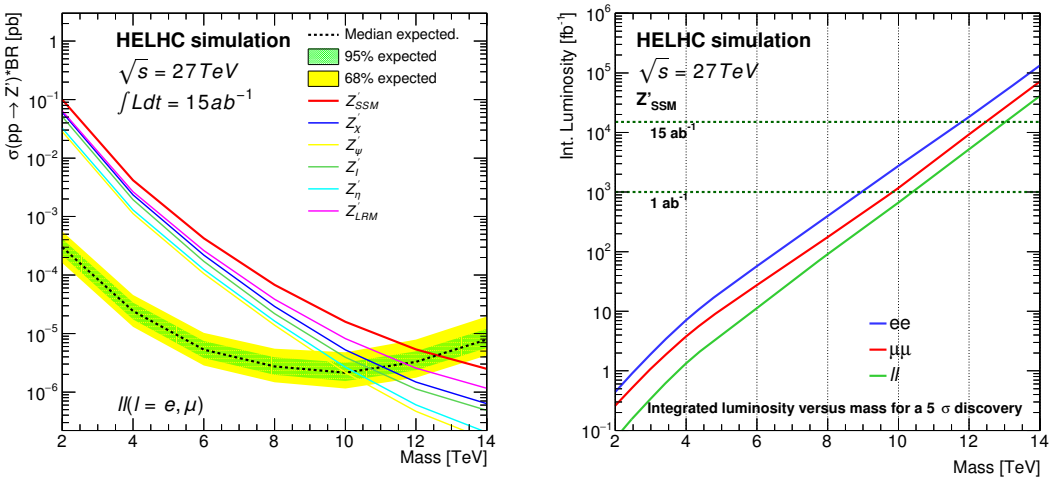

Figure 5: Limit versus mass for the di-lepton channel (left) and luminosity for a 5σ discovery (right) for the ee and $\mu\mu$ combined channels.

The variable A_{FB} can be seen as a measure of the charge asymmetry

$$A_{FB} = A_C = \frac{\sigma(\Delta|y| > 0) - \sigma(\Delta|y| < 0)}{\sigma(\Delta|y| > 0) + \sigma(\Delta|y| < 0)} \tag{2}$$

where $\Delta|y| = |y_l| - |y_{\bar{l}}|$. It has been checked that this definition is equivalent to defining

$$A_{FB} = \frac{\sigma_F - \sigma_B}{\sigma_F + \sigma_B} \tag{3}$$

with $\sigma_F = \sigma(cos\theta^*_{cs}) > 0$ and $\sigma_B = \sigma(cos\theta^*_{cs}) < 0$ and defining θ^* in the Collins-Soper frame as

$$cos\theta^*_{cs} = \frac{Q_z}{|Q_z|} \frac{2(P_l^+ P_{\bar{l}}^- - P_l^- P_{\bar{l}}^+)}{|Q|\sqrt{Q^2 + Q_T^2}} \tag{4}$$

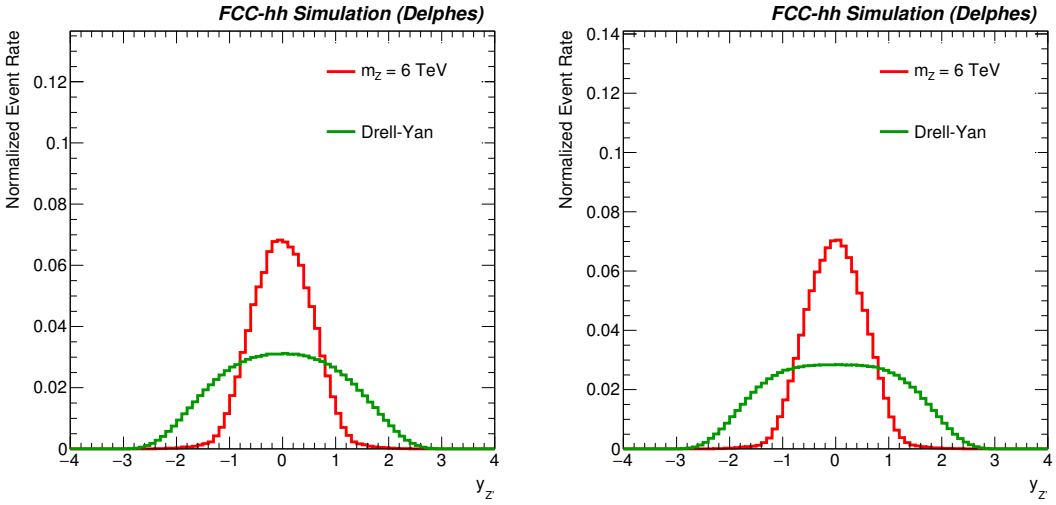

Figure 6: Z' rapidity distribution comparing a 6 TeV signal and Drell-Yan background for ee (left) and $\mu\mu$ channels (right).

	nominal		$\|\eta\| < 4.5$		no FSR		no ISR		Full interference	
Model	A_{FB}	r_y	A_{FB}	r_y	A_{FB}	r_y	A_{FB}	r_y	A_{FB}	r_y
SSM	6.62	6.09	6.62	6.09	6.62	6.09	6.62	6.09	6.62	6.09
LRM	6.39	6.09	6.62	6.09	6.62	6.09	6.62	6.09	6.62	6.09
ψ	6.10	6.09	6.62	6.09	6.62	6.09	6.62	6.09	6.62	6.09
χ	6.22	6.09	6.62	6.09	6.62	6.09	6.62	6.09	6.62	6.09
η	6.15	6.09	6.62	6.09	6.62	6.09	6.62	6.09	6.62	6.09
I	5.98	6.09	6.62	6.09	6.62	6.09	6.62	6.09	6.62	6.09

Table 2: A_{FB} and r_y values for different models and different assumptions.

where Q, Q_T and Q_z are the four-momentum, the transverse momentum, and the longitudinal momentum of the di-lepton pair. $P_l(P_{\bar{l}})$ represents the four momenta of the lepton (anti-lepton), and $P_l^{\pm} = (P_l^0 \pm P_l^3)$.

4.2.3 Optimisations

4.2.4 Results

TODOBEGING
show cross section versus int luminosity, show error on AFB ry for models (2D), show scan lumi for hard to distinguish model, table that shows this impact of the eta, ISR, FSR, etc... plot that shows how AFB and ry evolves with the deltaM cut Show the effect of a cut a different cut on ry TODOEND

We have checked that increasing the acceptance of the leptons to 4.5 in pseudo-rapidity did not improved the discrimination further. Using a profile likelihood technique, the signal strength μ can be fitted together with its corresponding error.

4.3 Hadronic analysis

In this section the hadronic decays of the Z' will be tested in order to enhance the discrimination potential.

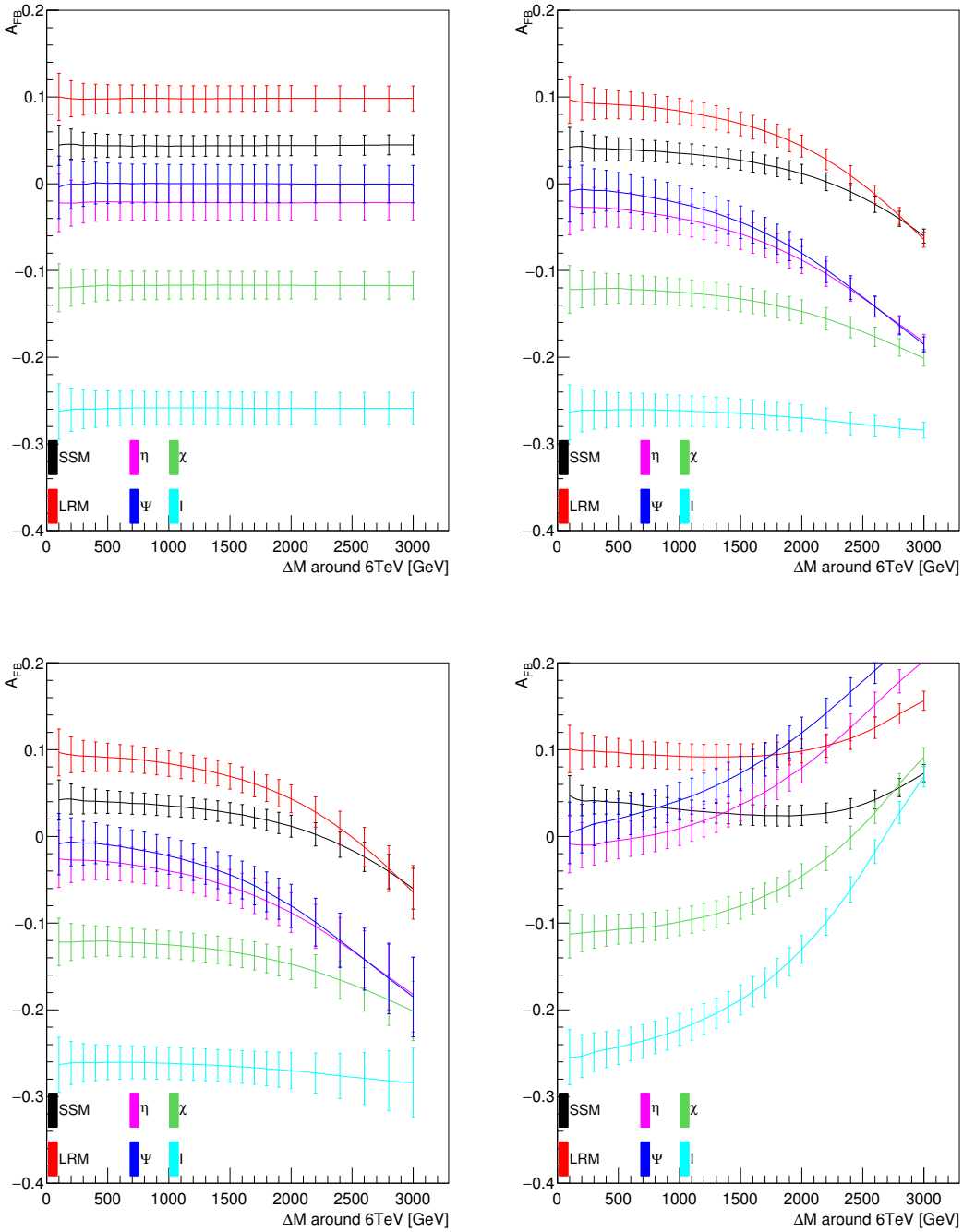

Figure 7: A_{FB} versus invariant mass range around 6TeV considering no backgrounds (top left), backgrounds with no uncertainties (top right), backgrounds with 10% uncertainties (bottom left) and full interference (bottom right).

4.3.1 $Z' \to t\bar{t}$

4.3.2 $Z' \to b\bar{b}$

4.3.3 $Z' \to q\bar{q}$

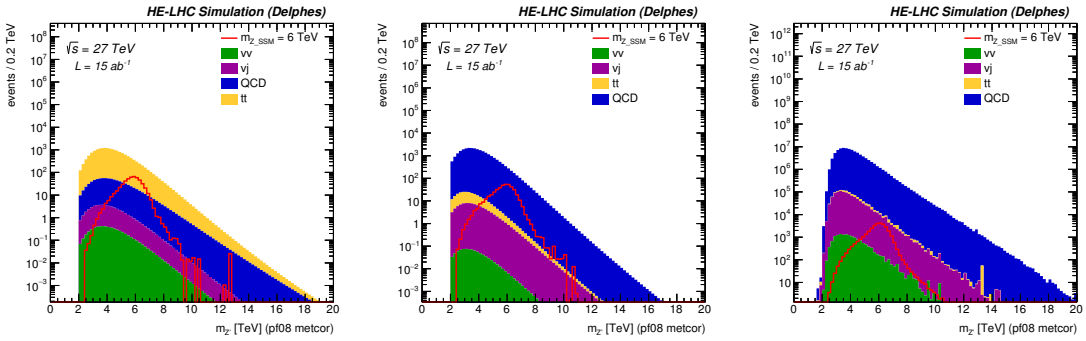

Figure 8: Left, center: Invariant mass for a 6 TeV signal after full event selection for ee channel (left) and $\mu\mu$ channel (center). Right: Transverse mass for a 6 TeV signal after full event selection for the $\tau\tau$ channel.

4.3.4 Results

The model discrimination achieved by the hadronic analyses for 4, 6 and 8TeV considering an integrated luminosity of 5, 15 and 30ab^{-1} respectively is shown on Fig. **??**, **??**, 9. From the leptonic analysis 4.2.1, it was shown that for r_y For all cases, except for a mass of 8TeV and an integrated luminosity of 5ab^{-1}, discrimination is obtained at more than one sigma for the di-jet case.

5 Summary

Acknowledgements

This work was supported by the Department of Energy, Contract DE-AC02-76SF00515.

References

[1] T. G. Rizzo, Phys. Rev. D **89**, no. 9, 095022 (2014) doi:10.1103/PhysRevD.89.095022 [arXiv:1403.5465 [hep-ph]].

[2] T. Han, P. Langacker, Z. Liu and L. T. Wang, arXiv:1308.2738 [hep-ph].

[3] L. A. Harland-Lang, A. D. Martin, P. Motylinski and R. S. Thorne, Eur. Phys. J. C **75**, no. 5, 204 (2015) doi:10.1140/epjc/s10052-015-3397-6 [arXiv:1412.3989 [hep-ph]].

[4] M. Aaboud *et al.* [ATLAS Collaboration], JHEP **1710**, 182 (2017) doi:10.1007/JHEP10(2017)182 [arXiv:1707.02424 [hep-ex]].

[5] A. M. Sirunyan *et al.* [CMS Collaboration], arXiv:1803.06292 [hep-ex].

[6] J. Han [ATLAS and CMS Collaborations], PoS ICHEP **2016**, 677 (2016).

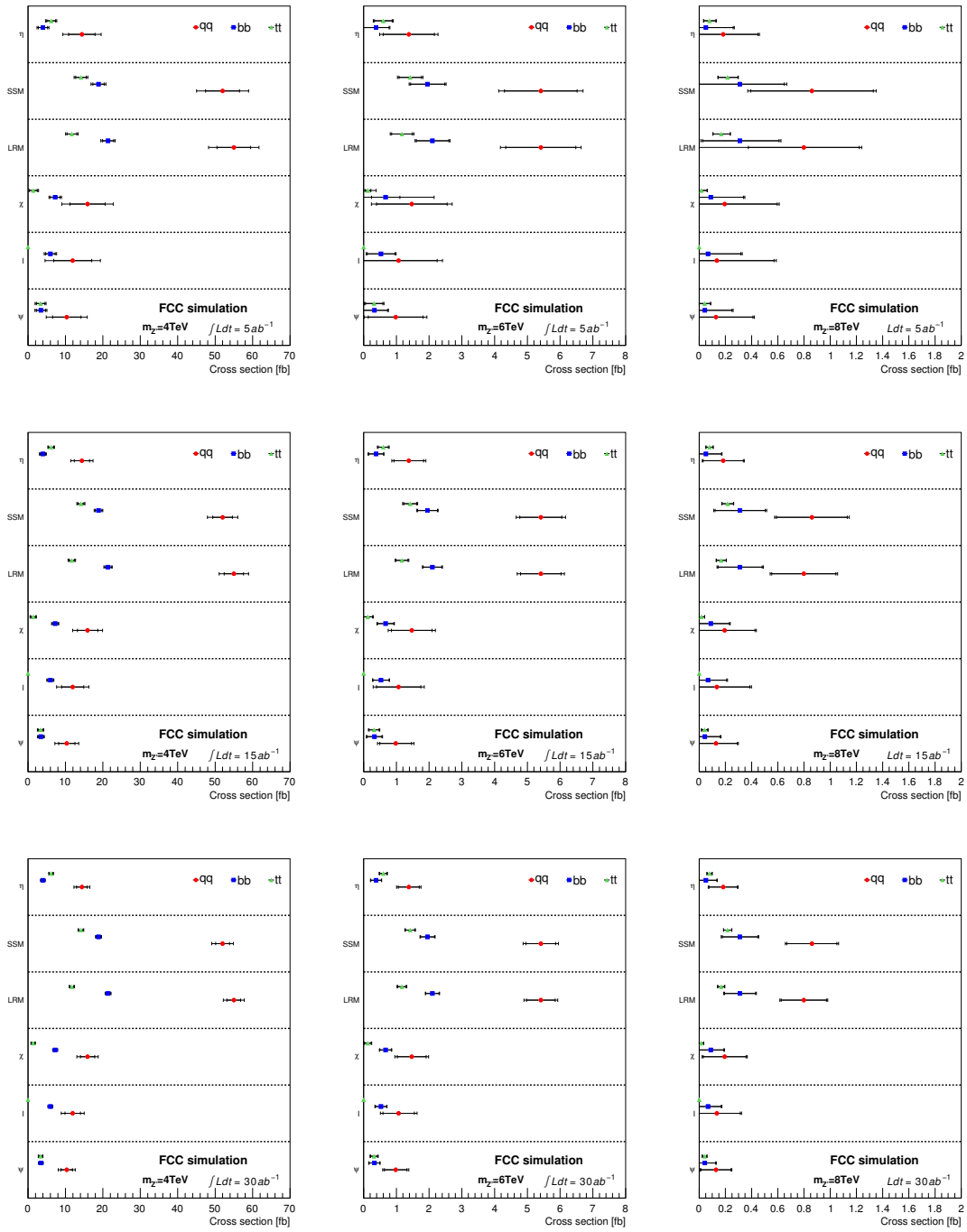

Figure 9: Discrimination for 4, 6 and 8TeV (left, center, right) masses with 5, 15 and 30ab^{-1} (up, middle, down) of integrated luminosity. Statistical and full uncertainties are shown on each point.

[7] CMS Collaboration [CMS Collaboration], CMS-PAS-SMP-16-007.

[8] FCCSW main page, http://fccsw.web.cern.ch/fccsw/

[9] HE-LHC twiki https://twiki.cern.ch/twiki/bin/view/LHCPhysics/HLHELHCWorkshop

[10] T. Sjstrand *et al.*, Comput. Phys. Commun. **191** (2015) 159 doi:10.1016/j.cpc.2015.01.024 [arXiv:1410.3012 [hep-ph]].

[11] J. Alwall *et al.*, JHEP **1407** (2014) 079 doi:10.1007/JHEP07(2014)079 [arXiv:1405.0301 [hep-ph]].